Kinetic Characterization of Phosphotransfer between CheA and CheY in the Bacterial Chemotaxis Signal Transduction Pathway†

Richard C. Stewart*

Department of Microbiology and Program in Molecular and Cellular Biology, University of Maryland, College Park, Maryland 20742

Received September 9, 1996; Revised Manuscript Received December 5, 1996⊗

ABSTRACT: Phosphorylation of the CheY protein is a crucial step in the chemotaxis signal transduction pathway of *Escherichia coli*. CheY becomes phosphorylated by acquiring a phosphoryl group from CheA, an autophosphorylating protein kinase. In this study, we utilized a rapid-quench instrument to investigate the kinetics of phosphotransfer in single-turnover experiments. Our results are consistent with a three-step mechanism for the CheA-to-CheY phosphotransfer reaction: (i) reversible binding of CheY to P-CheA; (ii) rapid, reversible phosphotransfer to CheY; (iii) reversible dissociation of the resulting CheA·CheY-P complex. Investigation of the effect of CheY concentration on the observed rate of phosphotransfer demonstrated saturation kinetics; the extrapolated limiting rate constant for phosphotransfer was 650 ± 200 s^{-1}, while the K_m value indicated from this work was 6.5 ± 2 μM. We demonstrated that the CheA−CheY phosphotransfer reaction was reversible by observing partial transfer of [^{32}P]phosphate from CheY-P to CheA and by observing the effect of high concentrations of unphosphorylated CheA on the equilibrium: P-CheA + CheY ↔ CheA + CheY-P. We found that the rate of phosphotransfer from P-CheA to CheY can be inhibited by unphosphorylated CheA as well as by a fragment of CheA (CheA$^{124-257}$) that contains the CheY binding site; these results suggest that the unphosphorylated form of CheA can effectively compete with P-CheA for available CheY (K_d ∼ 1.5 ± 0.6 μM for the CheY·CheA$^{124-257}$ complex and for the CheY·CheA complex).

The chemotaxis system of motile bacteria enables individual swimming cells to control their movements such that they migrate toward environments containing higher concentrations of chemoattractants and away from areas where the concentrations of chemorepellents are increasing (Berg & Brown, 1972). This directed movement results from the ability of the chemotaxis signal transduction pathway to control the direction of flagellar rotation over an appropriately rapid time scale, such that cells detect and respond to changes in extracellular concentrations of attractants/repellents within approximately a tenth of a second (Block et al., 1982; Khan et al., 1993; Segall et al., 1982). The components of the chemotaxis signal transduction pathway of *Escherichia coli* and *Salmonella typhimurium* have been identified and studied at a biochemical level (Bourret et al., 1991; Stock & Surette, 1996). As a result of such studies, we know that this pathway involves a small set of interacting cytoplasmic proteins (CheA, CheW, CheY, CheZ, CheR, and CheB) that enable four distinct transmembrane receptor proteins (Tsr, Tar, Trg, and Tap) to communicate with the flagellar motor.

The major role of these cytoplasmic signaling proteins is to regulate the level of phosphorylated CheY. The phosphorylated form of CheY (CheY-P)[1] interacts directly with the flagellar motor to control a cell's swimming pattern (Bourret et al., 1990; Welch et al., 1994). CheY-P is generated when CheY interacts with the phosphorylated form of CheA (Hess et al., 1988c; Wylie et al., 1988). CheA is an autophosphorylating protein kinase that catalyzes transfer of the γ-phosphoryl group of ATP to His-48 of the CheA protein (Hess et al., 1988b). The CheA-to-CheY phosphotransfer reaction then results in transfer of the phosphoryl group from CheA to Asp-57 of CheY (Sanders et al., 1989). The level of CheY-P present at any given time reflects not only the rate of CheY phosphorylation but also the rate of its dephosphorylation. CheY dephosphorylation is catalyzed by CheY itself in a relatively slow reaction (k ∼ 0.04 s^{-1}) but occurs much more rapidly in the presence of CheZ, which either operates as a phosphatase or enhances CheY's intrinsic autophosphatase activity (Hess et al., 1988a; Lukat et al., 1991; Huang & Stewart, 1993).

The chemotaxis receptor proteins sample the cell's local chemical environment and control the intracellular level of CheY-P accordingly. This control is accomplished, at least in part, by the receptors' ability to regulate the autokinase activity of CheA (Borkovich et al., 1988, 1989). CheW serves as a coupling factor that enables this regulation by enabling the chemotaxis receptor proteins to form a complex with CheA (Borkovich et al., 1989, 1990; Gegner et al., 1992). CheR and CheB are responsible for methylating and demethylating, respectively, the receptor proteins in a manner that further adjusts CheA autokinase activity to enable sensory adaptation (Borkovich et al., 1992; Ninfa et al., 1991). Thus, signaling in this system results from regulation of the intracellular level of CheY-P by the chemotaxis receptor proteins which themselves are controlled by the presence of attractant/repellent ligands as well as by methyl-

† This research was supported by NIH Grant GM52853 to R.C.S.

* To whom correspondence should be addressed. Telephone: 301-405-5475. Email: rstewart@microb.umd.edu.

⊗ Abstract published in *Advance ACS Abstracts,* February 1, 1997.

[1] Abbreviations: BSA, bovine serum albumin; CheY-P, phospho-CheY; DTT, dithiothreitol; IPTG, isopropyl β-D-thiogalactopyranoside; PAGE, polyacrylamide gel electrophoresis; P-CheA, phospho-CheA; P_i, inorganic phosphate; SDS, sodium dodecyl sulfate; TCA, trichloroacetic acid.

S0006-2960(96)02261-1 CCC: $14.00

ation/demethylation. Such regulation of CheY-P levels could result from receptors controlling the rate of CheA autophosphorylation, the rate of CheA−CheY phosphotransfer, and/or the rate of CheY dephosphorylation. At the level of cell behavior, the net result of such control is a system that supports rapid changes of swimming pattern in response to small changes of attractant/repellent concentrations even when these small changes are superimposed on high background levels of attractant/repellent (Berg & Tedesco, 1975).

The chemotaxis system is one of a large number of related signal transduction pathways that are collectively referred to as two-component signaling systems (Parkinson & Kofoid, 1992). Each such system utilizes a histidine protein kinase (homologous to CheA) that directs phosphorylation of a cognate response regulator protein (homologous to CheY). Understanding the details of the CheA−CheY phosphotransfer reaction may provide insights useful for studying these many other systems. In addition, detailed study of the chemotaxis system presents an excellent opportunity to uncover the molecular strategies by which a signal transduction circuit can achieve rapid responses and high sensitivity while maintaining the ability to integrate information and to adapt when stimulus levels cease to change. The first attempts to construct computer models of the chemotaxis signaling system have yielded some insights (Bray & Bourret, 1995; Hauri & Ross, 1995); however, understanding the molecular mechanism of signaling and adaptation in the chemotaxis system will require detailed knowledge of the kinetics of the phosphorylation and dephosphorylation reactions. The kinetics of the CheA autophosphorylation reaction have been explored in previous work (Borkovich & Simon, 1990; Surette et al., 1996; Tawa & Stewart, 1994), but little kinetic information is available for the other phosphotransfer and dephosphorylation reactions of the chemotaxis system. Here we report the results of kinetic characterization of the CheA−CheY phosphotransfer reaction, and we describe a minimal reaction scheme consistent with our observations. When considered in conjunction with the recent characterization of phosphotransfer from VanS to VanR (Fisher et al., 1996), our findings may help to define some of the common features of the phosphotransfer reaction mechanisms that operate in two-component sensory response systems.

MATERIALS AND METHODS

General Methods. High-purity ATP was purchased from Boehringer Mannheim. [γ-^{32}P]ATP and [^{32}P]orthophosphate were purchased from DuPont NEN. All other chemicals were reagent grade and were purchased from standard commercial sources. CheA and CheY were purified following previously published procedures (Wolfe & Stewart, 1993). CheA was stored in TEGDK buffer (Hess et al., 1988) at −80 °C and dialyzed against TEDKM buffer (Tawa & Stewart, 1995) before use. CheY was stored in TEDK buffer at −80 °C; $MgCl_2$ was added to CheY samples to give a final concentration of 10 mM before use in kinetic experiments. Concentrations of purified proteins were determined spectrophotometrically using extinction coefficients calculated following the method of Gill and von Hippel (1989): CheA, $\epsilon = 16.3$ mM^{-1} cm^{-1}; CheY, $\epsilon = 8.25$ mM^{-1} cm^{-1}. For CheA,$^{124-257}$ which lacks tryptophan residues and tyrosine residues and therefore is not amenable to such a calculation, protein concentration was determined using the BCA assay kit from Pierce Chemical Co. ^{32}P-CheA was generated and isolated as described by Hess et al. (1988) with two modifications: glycerol was omitted from the buffer, and the final P-CheA fraction (~2 mL) isolated from the gel filtration column was subjected to dialysis (2 changes of 500 mL of TKED buffer at 0−4 °C) before storing at −20 °C. The concentration of CheA in these samples was determined spectrometrically. This value, in conjunction with the specific activity of the ATP used in the labeling reaction, enabled calculation of the fraction of CheA that was phosphorylated (consistently 16% using our standard labeling conditions) when aliquots of the labeled samples were subjected to liquid scintillation counting. The concentrated ^{32}P-CheA samples (typically >5 μM) were diluted into TKED buffer, and $MgCl_2$ was added to give a final concentration of 10 mM immediately before use in kinetic experiments. TKED buffer contained 50 mM Tris-HCl, pH 7.5, 50 mM KCl, 0.5 mM EDTA, and 0.5 mM DTT. Acetyl [^{32}P]phosphate was synthesized as described by McCleary and Stock (1994).

Bacterial Strains and Plasmids. *E. coli* strain RP3098 [Δ(*flhA-flhD*), kindly provided by J. S. Parkinson, University of Utah] is a K12 derivative which expresses no chemotaxis proteins. This strain was used as the host for plasmid-directed overproduction of CheA and CheA.$^{124-257}$ Plasmids pAR1:cheA (Wolfe & Stewart, 1993) and pTM22 (Morrison & Parkinson, 1994) directed expression of high levels of wild-type CheA and CheA,$^{124-257}$ respectively, in response to IPTG induction. Strain BL21(DE3) (Studier et al., 1990) was used as the host for high-level expression of CheY using plasmid pT7:cheY [pET11a (from Novagen) into which the *cheY* gene had been inserted appropriately downstream of the T7 promoter]. Ampicillin was added to 100 μg mL^{-1} during growth of cell/plasmid cultures.

Rapid-Quench Experiments To Monitor Phosphotransfer Time Courses. The quench-flow apparatus was calibrated by monitoring the base-catalyzed hydrolysis of *p*-nitrophenylacetate (Gutfreund, 1969) as recommended by the instrument manufacturer (BioLogic). All phosphotransfer experiments were carried out in TKMD buffer (50 mM Tris-HCl, pH 7.5, 10 mM $MgCl_2$, 0.5 mM DTT, and 50 mM KCl) at a temperature of 25 °C (except where indicated otherwise) maintained by a circulating water bath. All protein samples contained 10 mM $MgCl_2$. For most quench-flow experiments, 60 μL of ^{32}P-CheA (typical concentration before mixing 0.1 μM) was mixed with 60 μL of CheY (concentrations ranging from 0.1 to 16 μM) in a BioLogic QFM5 Quench-Flow instrument. The resulting reaction mixture was allowed to age for a specified time interval before rapid quenching, which was accomplished by mixing the 120 μL reaction mixture with 120 μL of quench buffer (10% SDS, 0.1 M EDTA, and 50 mM Tris-HCl, pH 6.8); 100 μL of the resulting quenched samples was then mixed with 40 μL of 4× SDS−PAGE sample buffer, and then 20 μL of these samples was loaded onto 17% SDS−PAGE gels (loading every other lane) which were then run immediately for 45 min in a BioRad MiniProtean II apparatus at 170 V using running buffer that had been prechilled to 4 °C. Gels (not dried) were immediately sealed in plastic Seal-A-Meal bags and exposed to phosphoimager screens for 4 h. The number of counts in each band ([^{32}P]P_i, ^{32}P-CheY, and ^{32}P-CheA) was determined using a phosphoimager (BioRad). Actual concentrations of the radioactive species were calculated from the number of counts (arbitrary phosphoimager units) in a

particular gel band relative to the number of counts obtained for a known amount of ^{32}P-CheA (on the same gel) which was present in the 'zero time point' sample for each reaction set.

Reactions were performed at a series of CheY concentrations, and appropriate time points were obtained (a) by varying the speed of the step motors controlling flow of reactants and quenching solution through calibrated delay lines and (b) by varying the volume of the delay line. Each reaction was performed in at least two independent experiments, and for each time point, duplicate samples were generated and analyzed. The levels of P-CheA and CheY-P present in the duplicate samples were averaged and plotted as time courses. Observed rate constants were obtained by fitting each time course to a single exponential using the least-squares curve fitting function of an Applied Photophysics SX-17MV work station [Marquardt algorithm based on the Curfit routine of Bevington (1969)]. For each experiment, these fits provided two independent estimates of $k_{observed}$: one from fitting the time course of P-CheA disappearance, and one from fitting the time course of CheY-P appearance. The $k_{observed}$ values plotted in Figures 4 and 8 are averages of the values obtained for P-CheA disappearance and CheY-P appearance for at least two independent experiments, such that we obtained at least four estimates of each observed rate constant for each set of experimental conditions. The error bars in these plots represent the standard errors of the mean. For lower temperature studies, it was necessary to modify the composition of the quench buffer to 2% SDS, 50 mM EDTA, and 50 mM Tris-HCl, pH 6.8, to avoid precipitation.

For TCA quenching of samples, conditions were identical to those described above except that 10% TCA was used in place of the SDS, EDTA mixture and all samples contained 0.1 mg mL^{-1} BSA to serve as carrier protein. After 60 min on ice, TCA-quenched samples were centrifuged for 30 min in a microcentrifuge at 4 °C. Protein pellets were then washed with cold acetone before being dissolved in Laemmli sample buffer and subjected to electrophoresis.

Kinetic Simulations. Kinetic simulations (results shown as the solid lines in Figures 5, 7, and 8) were performed on a Macintosh SE/30 personal computer using the program Stella (High Peformance Systems, Inc.). These simulations utilized the reaction scheme presented in eq 3 (Discussion) and required input of values for each of the rate constants defined in this scheme: k_1, k_{-1}, k_2, k_{-2}, k_3, k_{-3}, k_4, k_{-4}. We set k_2 at 650 s^{-1} (an experimentally determined value); however, we had to make several assumptions to arrive at values for the remaining rate constants which could not be estimated directly from experimental measurements. For the purposes of these simulations, we assumed that a rapid equilibrium situation (Strickland et al., 1975) applied for all of the binding equilibria; i.e., we made the assumption that binding events (k_1, k_{-1}, k_3, k_{-3}, k_4, k_{-4}) were at least 10 times more rapid than the phosphotransfer steps (k_2 and k_{-2}). In addition, the values we assigned for these rate constants were chosen to maintain the ratios established by experimentally determined binding constants: $k_{-1}/k_1 = 6.5\ \mu$M (experimentally determined K_m; this work), $k_3/k_{-3} = 6.5\ \mu$M (Li et al., 1995), and $k_{-4}/k_4 = 1.5\ \mu$M (experimentally determined K_i; this work; Li et al., 1995). We then adjusted the k_{-2} value until the time courses and equilibrium end points reached in the simulations approximated those obtained experimentally (Figure 5). Best agreement was obtained using a value of 20 s^{-1} for k_{-2}. Further refinement of the optimal value of k_{-2} (to ~10 s^{-1}) was required by the results presented in Figure 7. All of the simulated time courses shown in Figures 5, 7, and 8 utilized this lower value for k_{-2}. Although the instability of CheY-P and the presence of unreactive P-CheA complicated our efforts to model the quantitative details of this system, the simulations indicated that the scheme presented in eq 3 can account for the main qualititative aspects of our experimental observations. Further experimental work will be necessary to determine whether the rapid equilibrium assumption is valid for this reaction and to provide better estimates of k_{-2} and the rate constants that govern the binding/dissociation events involving the various forms of CheA and CheY.

RESULTS

Monitoring the Time Course of Phosphotransfer from ^{32}P-CheA to CheY. Previous work demonstrated that phosphotransfer from P-CheA to CheY is complete within 5 s after mixing micromolar concentrations of these proteins. Five seconds is the fastest time point achievable using manual mixing. We sought conditions and procedures that would enable us to monitor the time course of this rapid reaction on a millisecond time scale. Therefore, we used a rapid-quench instrument to rapidly mix ^{32}P-CheA with CheY and then to halt the reaction at various appropriate time points by mixing the reactants with a quenching solution (SDS plus EDTA). We followed the disappearance of ^{32}P-CheA and the concomitant appearance of CheY-^{32}P through these time courses by subjecting the quenched mixtures to SDS−PAGE and by then using a phosphoimager to quantify the amount of each radiolabeled species in each time point sample. Before making extensive use of this approach to conduct detailed kinetic characterization of this reaction, we first addressed three basic questions:

(1) Were the quenching conditions effective in halting the reaction progress sufficiently rapidly such that the time courses would reflect the phosphotransfer reaction kinetics and not the quenching reaction kinetics?

(2) Did analysis of the A-to-Y phosphotransfer kinetics require that we take into account the ability of CheY-P to autodephosphorylate?

(3) Were the phosphohistidine linkage of P-CheA and the phosphoaspartate linkage of CheY-P stable during the quenching and SDS−PAGE procedures?

To address the first of these questions, we compared the time course observed using our standard quench conditions (5% SDS, 50 mM EDTA final concentrations after mixing) to that obtained using an alternative quenching condition (5% TCA final concentration after mixing). The similarity of these time courses (Figure 1A) indicated that the quenching reactions were sufficiently more rapid than the phosphotransfer reaction such that the observed time courses reflected phosphotransfer kinetics, not quenching kinetics (Gutfreund, 1969). Similar agreement between TCA-quenched and SDS, EDTA-quenched time courses was observed for CheY concentrations ranging from 0.05 to 8 μM CheY. At concentrations higher than 8 μM, the reaction becomes too rapid to measure using our instrument.

Within this range of CheY concentrations, we observed that the phosphotransfer reaction was complete in less than

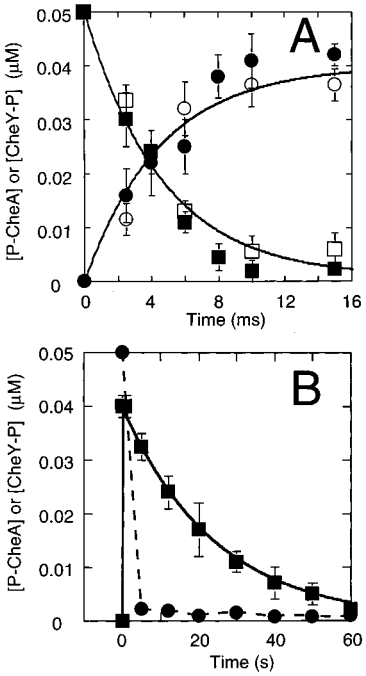

FIGURE 1: Effectiveness of quenching conditions and determination of appropriate time scale for observation of phosphotransfer from ^{32}P-CheA to CheY. (A) Comparison of SDS + EDTA and TCA as quenching agents. Phosphotransfer and quenching reactions were carried out as described under Materials and Methods using 0.05 μM ^{32}P-CheA and 5 μM CheY (concentrations after mixing). Time courses were obtained using 10% SDS, 0.1 M EDTA as quenching agent (■, P-CheA; ●, CheY-P) and for time courses obtained using 10% TCA as quenching agent (□, P-CheA; ○, CheY-P). Least-squares fitting of the time courses to single exponentials indicated that the rate constants were not significantly affected by the quenching conditions: SDS,EDTA-quenched samples indicated rate constants of 220 ± 40 and 200 ± 30 s^{-1} for disappearance of P-CheA and appearance of CheY-P, respectively; TCA-quenched samples indicated rate constants of 210 ± 40 and 250 ± 50 s^{-1} for disappearance of P-CheA and appearance of CheY-P, respectively. TCA-quenched time courses were corrected to account for a hydrolysis of the protein phosphoryl groups resulting from the necessary prolonged exposure to acidic conditions. Solid lines represent simulated exponential time courses using rate constants of 215 and 225 s^{-1} for disappearance of P-CheA and appearance of CheY-P, respectively. (B) Reaction time courses extended to longer times. Time courses for the reaction between 0.05 μM P-CheA and 5 μM CheY were collected out to 60 s (using SDS, EDTA quenching): ■, CheY-P; ●, P-CheA.

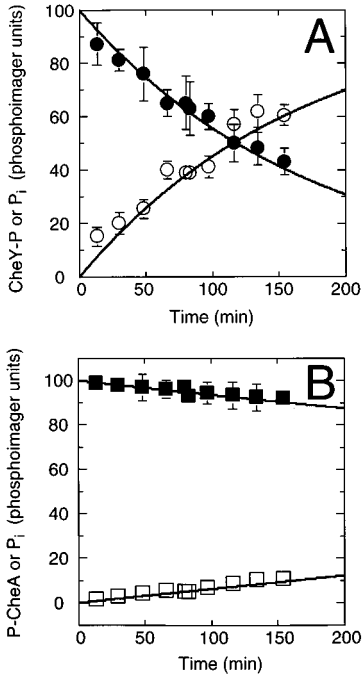

FIGURE 2: Stability of CheY-P and P-CheA during SDS−PAGE. (A) To assess the stability of CheY-P, a single quench-flow sample containing ~0.05 μM CheY-^{32}P and <0.002 μM ^{32}P-CheA was divided into 10 μL aliquots which were loaded onto a 17% SDS−PAGE gel (pH 8.8) and subjected to electrophoresis for intervals ranging from 15 to 180 min. Gels were analyzed using a phosphoimager as described above to quantify the relative levels of CheY-^{32}P (●) and $[^{32}P]_i$ (○) present at each time point. (B) A similar experiment was performed using aliquots containing ^{32}P-CheA (no CheY-^{32}P) to assess the stability of the phosphohistidine linkage of CheA: (■) ^{32}P-CheA and (□) $[^{32}P]P_i$. These experiments demonstrated progressive loss of CheY-P and P-CheA (with concomitant production of P_i). Time courses were fit to single exponentials by least-squares analysis (solid lines indicate the time courses predicted for these fits). Additional experiments indicated that hydrolysis of P-CheA and CheY-P did not occur to any appreciable extent during prolonged incubation in the SDS, EDTA quench buffer: i.e., hydrolysis of the phosphoprotein linkage occurred during electrophoresis, not during storage in sample buffer over these intervals.

a second. When we extended the time range out to 60 s (Figure 1B), we observed a slow exponential decrease in CheY-P. The rate constant describing this decrease (0.045 s^{-1}) was consistent with the value determined previously for autodephosphorylation of CheY-P (Hess et al., 1988a; Lukat et al., 1991). Thus, the autodephosphorylation reaction was over 1000 times slower than the phosphotransfer reaction and did not affect the levels of CheY-P observed over the short time intervals needed for completion of phosphotransfer from CheA to CheY. The long time courses indicated that a small percentage (2−4%) of the P-CheA in our preparations did not transfer its phosphoryl group to CheY even at extended times. This residual level of P-CheA remained even though CheY was present in excess over P-CheA and despite the fact that unphosphorylated CheY was being regenerated as a result of the autodephosphorylation reaction; 94−98% of the P-CheA became dephosphorylated within a few tenths of a second of mixing P-CheA with CheY. Following this rapid reaction, the level of P-CheA appeared to decrease slightly over the time range from 5 to 60 s, but this change was very small (1−3% of the total P-CheA level). The nature of the nonreactive P-CheA remains unclear, and its presence complicated efforts to quantitatively describe the following equilibrium: P-CheA + CheY ↔ CheA + CheY-P.

Previous work had demonstrated that the phosphoaspartate linkage in CheY-P hydrolyzes at an appreciable rate even when the protein has been denatured (Lukat et al., 1991; Stock et al., 1988). Similar studies indicated the relative stability of the phosphohistidine linkage in P-CheA under conditions of neutral and basic pH (Wylie et al., 1988). To assess the effect of our SDS−PAGE conditions on the stability of the phosphoprotein linkages of CheA and CheY, we subjected aliquots of a CheY-^{32}P sample and aliquots of a ^{32}P-CheA sample to electrophoresis for varying time intervals and then measured how much of the ^{32}P label remained associated with the phosphoprotein and how much was hydrolyzed to generate $[^{32}P]_i$. The results of these experiments (Figure 2) incidated hydrolysis of CheY-P with a $t_{1/2}$ of 115 ± 20 min and hydrolysis of P-CheA with a $t_{1/2}$ of 1000 ± 100 min in the gels under our conditions (detailed under Materials and Methods). Thus, P-CheA was relatively

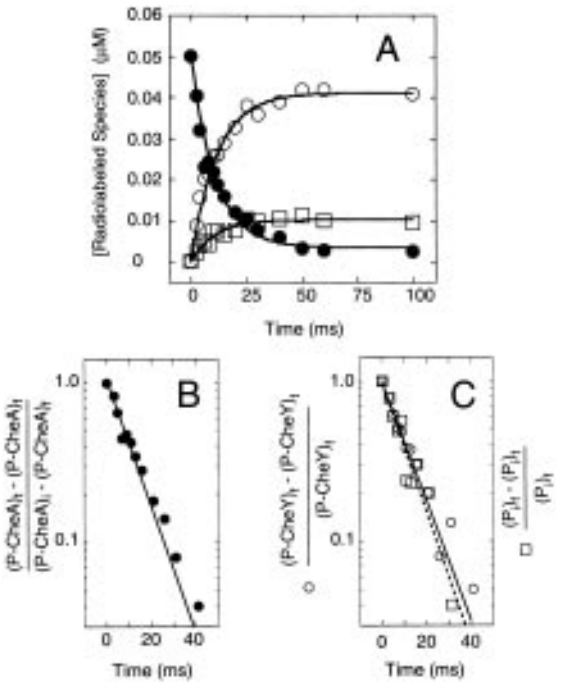

FIGURE 3: Time course of phosphotransfer from ^{32}P-CheA to CheY. ^{32}P-CheA was mixed with CheY in a quench-flow instrument, and the phosphotransfer reaction was allowed to proceed for the indicated times before quenching (SDS + EDTA). Samples were subjected to SDS−PAGE, and the gels were analyzed using a phosphoimager as described under Materials and Methods. Initial concentrations of the reactants (after mixing) were 0.05 μM P-CheA and 1.0 μM CheY. Each data point represents the average of two replicates for a single experiment: (●) P-CheA; (○) CheY-P; (□) P_i. Lines represent computer-generated least-squares fits of the data to single exponential curves. (A) Time courses plotted as [Radiolabeled Species] versus time; (B and C), semilog plots of the data presented in (A).

stable during electrophoresis: only a few percent hydrolysis occurred during our standard 45 min electrophoretic runs. By contrast, the relative instability of CheY-P during electrophoresis resulted in hydrolysis of ~20% of the CheY-P during our standard 45 min electrophoretic runs. While this loss is not expected to influence the values of the observed rate constants for the phosphotransfer reactions (since the relative amount of hydrolysis would be approximately the same for each sample in a given time course), it did limit the accuracy of determining the end point concentrations of the phosphorylated species.

Kinetics of Phosphotransfer from ^{32}P-CheA to CheY. Using the procedures described above, we monitored: (i) the disappearance of ^{32}P-CheA, (ii) the appearance of CheY-^{32}P, and (iii) the appearance of inorganic phosphate for time courses that were sufficiently long to allow the rapid phosphotransfer reaction to reach completion (i.e., 50−1000 ms, depending on the CheY concentration). For each of the radiolabeled species, we observed a simple exponential time course over this time scale (Figure 3A). Semilog plots of these time courses were linear for over 3 half-lives, and we observed no evidence of biphasicity (Figure 3 B,C). Least-squares fitting of each time course to a single exponential was used to extract the associated pseudo-first-order rate constant. The time course of P-CheA disappearance was mirrored by the appearance of P-CheY and inorganic phosphate: essentially the same rate constant (within experimental error) described all three time courses. The appearance of inorganic phosphate on this rapid (millisecond) time scale raised the possibility that P_i was being generated by very rapid hydrolysis of the CheY phosphoryl group and/or the CheA phosphoryl group, perhaps analogous to that observed by Fisher et al. (1996) in their investigation of phosphotransfer from VanS to the response regulator VanR. However, careful analysis of the stability of P-CheA and CheY-P during SDS−PAGE (Figure 2) indicated that the $[^{32}P]_i$ was being generated primarily by hydrolysis of CheY-P during electrophoresis: $[^{32}P]_i$ was not generated on the rapid time scale of the phosphotransfer reaction. This conclusion is consistent with our observation that, under a variety of different temperature and concentration conditions, the apparent rate of phosphate appearance was always approximately the same as the rate of P-CheY generation and that the level of $[^{32}P]P_i$ was consistently 20−25% of the level of ^{32}P-CheY under our gel conditions. Because the P_i was not generated as a direct result of the P-CheA·CheY interaction, we did not consider it further in our analysis.

We were interested in determining whether the rate of phosphotransfer from P-CheA to CheY was affected by the CheY concentration in a saturable manner that would indicate formation of a P-CheA·CheY complex prior to the chemical step responsible for phosphotransfer. To address this question, we determined the values of the pseudo-first-order rate constants describing the reaction time courses when 0.025 μM ^{32}P-CheA was mixed with a series of CheY concentrations ranging from 0.125 to 8 μM; these reactions were all performed at 25 °C. Analysis of these results in the form of a double-reciprocal plot appeared to indicate saturation kinetics (Figure 4A), however, the *y*-intercept of the double-reciprocal plot (see Figure 4A inset) was quite close to the origin. A *y*-axis intercept for this plot at the origin would have indicated a simple second-order reaction; i.e., the data would not provide any evidence for the existence of a P-CheA·CheY complex. Because of the potential ambiguity in interpreting this crucial point, we sought further experimental evidence to determine whether the phosphotransfer reaction should be regarded as a second-order reaction or as a multistep reaction whose rate is saturable at high CheY concentration. We were unsuccessful in monitoring phosphotransfer kinetics at CheY concentrations higher than 8 μM because the reaction was too rapid [near-completion at the earliest accessible time point (2.5 ms)]. To further address the question of saturation kinetics, we lowered the reaction temperature to 8 °C (the lowest temperature we could maintain reproducibly in our rapid quench instrument) and monitored reaction time courses at a series of higher CheY concentrations (2−25 μM) interacting with a fixed concentration of ^{32}P-CheA. Analysis of the results of these lower temperature experiments (Figure 4B) clearly demonstrated saturation kinetics and suggested that the phosphotransfer reaction involved formation of a P-CheA·CheY complex prior to a chemical step that results in transfer of the phosphoryl group from CheA to CheY (eq 1). This phosphotransfer step (k_2) became rate-limiting at saturating concentrations of CheY.

$$\text{P-CheA} + \text{CheY} \underset{k_{-1}}{\overset{k_1}{\rightleftharpoons}} \text{P-CheA·CheY} \xrightarrow{k_2} \text{CheA} + \text{CheY-P} \quad (1)$$

The rate constant (k_2) for the phosphotransfer step (i.e., the apparent first-order rate constant at extrapolated saturating

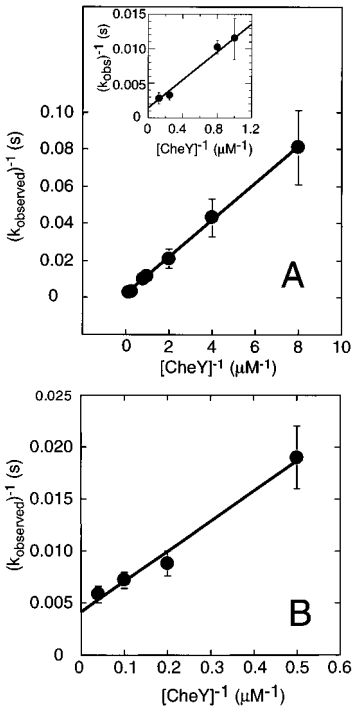

FIGURE 4: Effect of CheY concentration on kinetics of phosphotransfer. Reactions contained 0.025 μM P-CheA and CheY at a series of concentrations that would maintain pseudo-first-order conditions. (A) Double-reciprocal plot of the observed pseudo-first-order rate constant (k_{obs}) as a function of CheY concentration for phosphotransfer reactions at 25 °C. The inset shows the expanded scale at high CheY concentrations to demonstrate that the double-reciprocal plot intersects the *y*-axis just above the origin. (B) Double-reciprocal plot of the dependence of k_{obs} on CheY concentration for phosphotransfer for reactions at 8 °C. Solid lines in both panels indicate results of least-squares fitting of the data to a linear relationship (for the double-reciprocal plot). Error bars represent standard errors of the mean.

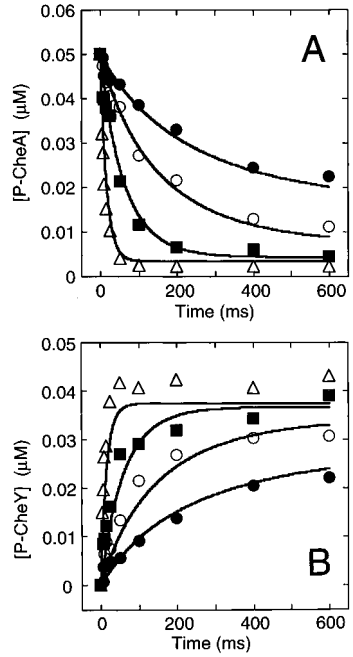

FIGURE 5: Effect of CheY concentration on the end point of the rapid phosphotransfer reaction. Reactions were monitored as described under Materials and Methods and contained 0.05 μM ^{32}P-CheA and CheY at 0.05 μM (●), 0.1 μM (○), 0.25 μM (■), or 1.0 μM (△). Each data point represents the average of two replicates for a single experiment. Solid lines represent computer simulations of time courses generated as described under Materials and Methods.

CheY concentration) was indicated by the reciprocal of the *y*-axis intercept in the plots of Figure 4A,B: ~650 ± 200 s^{-1} at 25 °C or ~250 ± 40 s^{-1} at 8 °C. The reciprocals of the *x*-axis intercepts in these plots (Figure 4A,B) defined a K_m value for the interaction of CheY with P-CheA (6.5 ± 2 μM at 25 °C; 7 ± 2 μM at 8 °C).

To extend our kinetic characterization of the interaction between CheY and P-CheA, we monitored reaction time courses after mixing a fixed concentration of ^{32}P-CheA (0.05 μM) with a series of lower CheY concentrations ranging from 0.05 to 1 μM (Figure 5). These results indicated that the final level of CheY-P increased progressively as the CheY concentration was increased and indicated that maximal removal of the CheA phosphoryl group did not occur unless the ratio of CheY to ^{32}P-CheA was greater than ~4. This observation suggested that the CheA−CheY phosphotransfer reaction was reversible and that the final levels of P-CheA and CheY-P at which the time courses plateaued were the result of an equilibrium situation.

Reversibility of CheA−CheY Phosphotransfer. The results presented in Figure 5 suggested that the CheA−CheY phosphotransfer reaction was reversible, although the overall equilibrium constant for the reaction strongly favored transfer of the CheA phosphoryl group to CheY. Previous work by Lukat et al. (1990) indicated reversibility of this phosphotransfer reaction under more unusual circumstances. We sought direct evidence that phosphotransfer from P-CheY to CheA was possible under our reaction conditions. We directly demonstrated such a reaction in two different experiments (Figure 6). In the first, we performed a double mixing experiment in the quenched-flow instrument: the first mixing event was used to generate CheY-^{32}P in the aging line of the instrument, and the second mixing event was then used mix this CheY-P with a high concentration of unphosphorylated CheA (5 μM final concentration); this final reaction mixture was then allowed to age for a series of intervals (from 5 ms to 200 ms) before quenching. The reaction products were subjected to SDS−PAGE followed by phosphoimager analysis as shown in Figure 6A. As 'zero time point controls' for this experiment, we replaced the unphosphorylated CheA solution (used in the second mixing event) with a buffer solution that contained no CheA. In the absence of this excess unphosphorylated CheA, the levels of P-CheA and CheY-P remained constant for all time points collected after the second mixing event (data not shown): i.e., the levels were the same as that shown in the "0 lane" of Figure 6A. These results demonstrated that the CheA added in the second mixing event resulted in production of a higher level of P-CheA at the final equilibrium end point. The time course for appearance of P-CheA in this experiment indicated that the new equilibrium level of P-CheA was reached fairly rapidly (within several hundred milliseconds), although we have not yet performed an extensive kinetic analysis of this reaction.

A second approach to demonstrating phosphotransfer from ^{32}P-CheY to CheA made use of the ability of CheY to autophosphorylate in the presence of acetyl phosphate (Lukat et al., 1992). CheY-^{32}P was generated by adding acetyl [^{32}P]-phosphate to CheY, and then CheA was added to this mixture and allowed to interact with the CheY-^{32}P for a short time before subjecting the sample to SDS−PAGE followed by

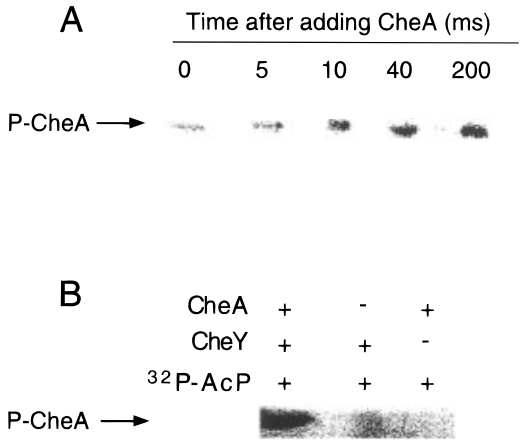

FIGURE 6: Phosphotransfer from P-CheY to CheA. (A) Phosphoimager image showing time course of [P-CheA] increase in the double-mixing experiment where CheY-P was generated in the first mixing event and then mixed with a high concentration of unphosphorylated CheA. The first mixing event initiated a reaction between 0.025 μM ^{32}P-CheA and 1 μM CheY; this reaction was allowed to proceed in the delay line for 600 ms before the reaction mixture was pushed into a second mixer that resulted in addition of 5 μM unphosphorylated CheA (concentration after mixing). The resulting reaction between CheY-P and CheA was allowed to proceed for the indicated time intervals (see numbers above corresponding lanes in gel) after the second mixing event and then quenched (SDS, EDTA). Samples were then subjected to SDS−PAGE. In this experiment, maximal sensitivity was required to detect the very low level of P-CheA generated, and so we were forced to dry the gels to enable prolonged exposure (24 h) of the gels to the phosphoimaging screen. The drying process allowed long exposure times without complications arising from diffusion of the proteins that occurs in a wet gel; however, drying destroyed a significant fraction of the CheY-P (through hydrolysis) and precluded quantifying small changes in the relatively large level of P-CheY (0.01 μM after mixing with CheA). The regions of the gel corresponding to CheY-P and acetyl phosphate were cropped from the image shown for the sake of clarity. (B) Phosphoimager image showing production of P-CheA when ~25 mM acetyl [^{32}P]-phosphate was added to 100 μM CheY followed by addition of unphosphorylated CheA (final concentration 25 μM) after first allowing CheY autophosphorylation to proceed for 30 s. The reverse phosphotransfer reaction was allowed to proceed for ~5 s before SDS−PAGE sample buffer was added to halt the reactions. Labels above the gel indicate components present in three different combinations of components in this experiment. For the reasons discussed above, the gel was dried prior to phosphoimager analysis, and the region of the gel corresponding to CheY-P and acetyl phosphate was removed from the image.

phosphoimager analysis. The results of this experiment (Figure 4B) demonstrated transfer of ^{32}P from acetyl phosphate to CheA only in the presence of CheY, a result consistent with phosphotransfer from P-CheY to CheA.

To incorporate this reversibility into our minimal reaction scheme, the simple model of eq 1 must be modified:

$$\text{P-CheA} + \text{CheY} \underset{k_{-1}}{\overset{k_1}{\rightleftharpoons}} \text{P-CheA}\cdot\text{CheY} \underset{k_{-2}}{\overset{k_2}{\rightleftharpoons}} \text{CheA}\cdot\text{CheY-P} \underset{k_{-3}}{\overset{k_3}{\rightleftharpoons}} \text{CheA} + \text{CheY-P} \quad (2)$$

The final reversible step in this scheme involves dissociation of a CheA·CheY-P complex. We have included this product dissociation step in eq 2 although the kinetic data presented up to this point do not require it. Results presented below support this inclusion. Li et al. (1995) measured a K_d of ~6.7 μM for the CheA·CheY-P complex that dissociates in this step.

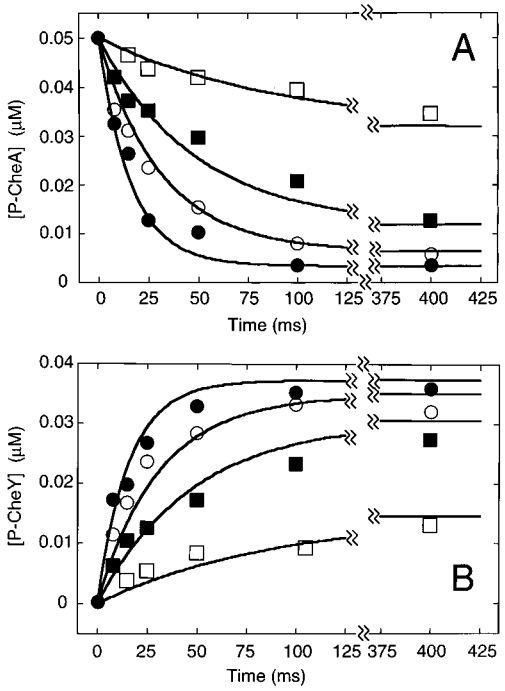

FIGURE 7: Inhibition of phosphotransfer by unphosphorylated CheA. Reactions contained 0.05 μM ^{32}P-CheA, 1 μM CheY, and unphosphorylated CheA at a series of concentrations: 0 (●), 2 μM (○), 5 μM (■), and 25 μM (□). The unphosphorylated CheA was added to the ^{32}P-CheA sample prior to loading the reactants into the quench-flow instrument. Samples were generated and analyzed as described under Materials and Methods. (A) Time course of disappearance of P-CheA. (B) Time course for appearance of CheY-P. Samples were collected and analyzed as described under Materials and Methods. Solid lines represent computer simulations of time courses generated using the phosphotransfer model of eq 3 as described under Materials and Methods.

The reaction scheme depicted in eq 2 predicted that the relative levels of CheY-P and P-CheA present at equilibrium should be sensitive to the concentration of unphosphorylated CheA. We tested this prediction by determining whether high levels of unphosphorylated CheA could affect the equilibrium end point of the phosphotransfer reaction when a fixed concentration of CheY was mixed with a fixed concentration of P-CheA. The results of these experiments (Figure 7) clearly demonstrated that the equilibrium levels of P-CheA and CheY-P were affected by high concentrations of unphosphorylated CheA. This finding is consistent with the idea that high concentrations of unphosphorylated CheA are capable of pushing the equilibrium of eq 2 further in the reverse direction, thus favoring a higher equilibrium concentration of P-CheA (lower equilibrium concentration of P-CheY).

Analysis of the time courses in Figure 7 indicated that high levels of unphosphorylated CheA also have the ability to inhibit the rate of approach to equilibrium following mixing of P-CheA with CheY. For example, in the absence of any "extra CheA", the phosphotransfer reaction in Figure 7 proceeded with an apparent rate constant of ~63 s^{-1}, while in the presence of 25 μM "extra CheA" the observed rate constant was ~13 s^{-1}. This inhibition was not predicted by the model presented in eq 2; however, previous work (Li et al., 1995) demonstrated that unphosphorylated CheA can bind to CheY fairly tightly (K_d 1−1.7 μM), and such an interaction would allow unphosphorylated CheA to compete with P-CheA for the available CheY. In theory, it is possible to

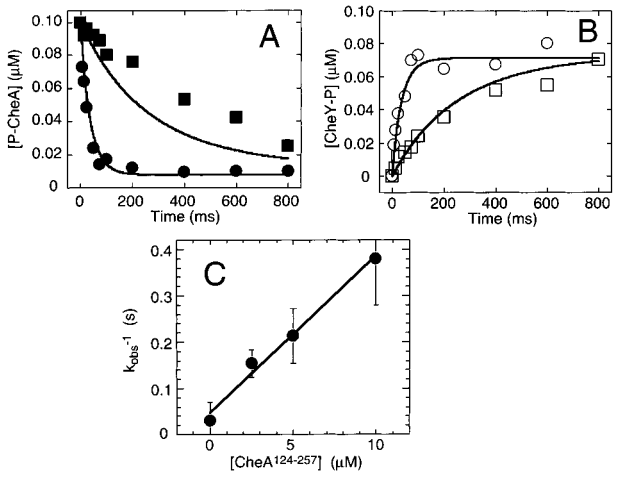

FIGURE 8: Inhibition of phosphotransfer from P-CheA to CheY by CheA.$^{124-257}$ Reactions contained 0.1 μM ^{32}P-CheA, 0.5 μM CheY, and CheA$^{124-257}$ ranging from 0 to 10 μM. Samples were collected and analyzed as described under Materials and Methods. CheA$^{124-257}$ was added to the ^{32}P-CheA sample prior to loading the reactants into the quench-flow instrument. (A) Time course of disappearance of P-CheA: (●) no CheA$^{124-257}$ added; (■) 10 μM CheA$^{124-257}$ added. (B) Time course for appearance of CheY-P: (○) no CheA$^{124-257}$ added; (□), 10 μM CheA$^{124-257}$ added. (C) Dixon plot of inhibition data. Solid lines in (A) and (B) represent computer simulations of time courses generated as described under Materials and Methods. Solid line in (C) represents computer-generated linear least-squares fit indicating a K_d of 1.5 μM for the CheY·CheA$^{124-257}$ complex. This K_d value is derived from the extrapolated x-axis intercept (K_i) of the Dixon plot assuming that CheA$^{124-257}$ acts as a competitive inhibitor of P-CheA and that the binding/dissociation events betwen CheY and CheA$^{124-257}$ are sufficiently more rapid than the CheA-to-CheY phosphotransfer step that a rapid equilibrium situation exists. In such a situation, $k_{obs} = k_0[K_i/(K_i + [I])]$, where k_0 is the observed rate constant in the absence of inhibitor (CheA$^{124-257}$). A plot of k_{obs}^{-1} versus [CheA$^{124-257}$] has an x-axis intercept equal to K_i.

extract a K_i (K_d) for the CheA·CheY interaction from the results in Figure 7, but computer modeling of this kinetic scheme indicated that such an analysis is complicated considerably by the ability of unphosphorylated CheA to participate in the reverse phosphotransfer reaction. Because of this complication, we decided to explore a somewhat simpler inhibition scheme before attempting a quantitative analysis of the results presented in Figure 7.

Inhibition of Phosphotransfer by CheA$^{124-257}$. For this simpler inhibition scheme, we used a fragment of CheA that comprises residues 124−257 of the full-length protein. This protein fragment spans the P2 domain of CheA (Morrison & Parkinson, 1994), a segment of the protein that contains the CheY binding site (Li et al., 1995; Swanson et al., 1993b). This CheA fragment lacks the autophosphorylation site (His-48) and the kinase active site determinants (Parkinson & Kofoid, 1992; Stock & Surette, 1996). CheA$^{124-257}$ has been demonstrated to bind CheY with approximately the same affinity as does the full-length CheA protein (Li et al., 1995). Thus, we expected that this CheA fragment would be capable of inhibiting phosphotransfer kinetics; however, because it cannot participate in the reverse phosphotransfer reaction, its effects on the phosphotransfer kinetics would not be as complicated as for the full-length CheA. We investigated the ability of CheA$^{124-257}$ to inhibit the P-CheA ↔ CheY phosphotransfer reaction (Figure 8). Our results indicated that this CheA fragment competed effectively with P-CheA for the available CheY. Assuming a simple competitive inhibition model, analysis of the effect of CheA$^{124-257}$ on the observed rate constant of phosphotransfer from P-CheA to CheY indicated a K_d (K_i) of approximately 1.5 ± 0.6 μM for the CheY·CheA$^{124-257}$ complex (Figure 8C). This value agreed with the K_d of the CheY·P2 complex determined by calorimetry (Li et al., 1995) and by spectrofluorometric titrations (McEnvoy et al., 1995; Shukla & Matsumura, 1995). High concentrations of CheA$^{124-257}$ had a minor effect on the equilibrium end point reached under these conditions, causing only a small increase in the equilibrium level of P-CheA. This increase indicated that the CheA$^{124-257}$ fragment must have an affinity for P-CheY that is somewhat lower that its affinity for unphosphorylated CheY, but that this difference is probably not greater than a factor of 10. This interpretation agreed with the results of calorimetric measurements of Li et al. (1995), who reported a 5−6-fold decrease in the affinity of the CheA·CheY interaction when CheY is phosphorylated.

We expected that full-length CheA could inhibit the phosphotransfer kinetics by binding to CheY in much the same way that CheA$^{124-257}$ did. Computer modeling of such an inhibition scenario supported this idea (see Figure 7). It is worth emphasizing that all of the experiments described in this paper were performed using ^{32}P-CheA that was generated by mixing CheA with a mixture of cold ATP and [γ-^{32}P]ATP and then separating the labeled P-CheA from the ATP by a combination of ammonium sulfate precipitation, gel chromatography, and dialysis. However, because of the nature of the CheA autophosphorylation reaction (a readily reversible equilibrium) (Hess et al., 1987; Surette et al., 1995; Tawa & Stewart, 1994), the "phosphorylated CheA" generated and isolated is necessarily a mixture of unphosphorylated CheA and P-CheA. This is true not only for the experiments reported here but also for all previously published work involving P-CheA. Our specific labeling/phosphorylation conditions generated a mixture of 16% P-CheA and 84% CheA (see Materials and Methods), so our standard reaction conditions included 0.05 μM P-CheA and 0.26 μM unphosphorylated CheA. Therefore, it was important for us to determine whether the kinetics we observed were affected by the presence of this level of unphosphorylated CheA. The results of Figure 7 indicated that unphosphorylated CheA inhibited the phosphotransfer kinetics by competing with P-CheA for the available CheY. Computer modeling of this kinetic scheme indicated that the dissociation constant for the CheA·CheY complex is ∼1.5 ± 0.6 μM. Thus, the low level of unphosphorylated CheA (0.26 μM) present in our standard reaction mixtures had only a minor effect on the kinetics of the reactions and on the final equilibrium end points reached.

Another property of CheA had the potential to influence the phosphotransfer kinetics: CheA can dissociate from a dimer to monomers at low protein concentration. Surette et al. (1996) used several independent approaches to measure a dissociation constant of 0.1−0.2 μM for CheA from *S. typhimurium*, and our own measurements indicated a similar value for the *E. coli* protein (0.1 μM, data not shown). Phosphorylation of CheA does not affect the monomer−dimer equilibrium of CheA (Surette et al., 1996). We investigated the possibility that the monomer/dimer status of P-CheA might affect the kinetics of phosphotransfer. We monitored the time course of phosphotransfer when 0.01 μM P-CheA (total CheA concentration 0.062 μM) was mixed

with 2 μM CheY and compared this time course to that generated when 0.1 μM P-CheA (total CheA concentration 0.62 μM) was mixed with 2 μM CheY. There were no significant differences in these time courses (data not shown), indicating that the phosphotransfer kinetics were not significantly affected by the monomer/dimer status of the P-CheA. Both P-CheA samples were incubated at room temperature for 60 min prior to the phosphotransfer reaction to allow for slow adjustments of monomer/dimer equilibrium; previous work by Surette et al. (1996) and others (Wolfe & Stewart, 1993; Swanson et al., 1993a) has demonstrated that this interval provides ample time for dissociation of CheA dimers.

DISCUSSION

Minimal Reaction Scheme Describing CheA−CheY Interactions. One goal of the kinetic studies summarized here was to construct a minimal reaction scheme that accounted for each of the CheA−CheY interactions that influence the phosphotransfer reaction:

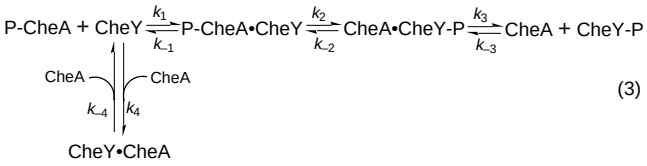

(3)

This scheme is consistent with each of the major observations made in this work: (i) saturation of the rate of phosphotransfer at high CheY concentrations; (ii) reversibility of the phosphotransfer reaction; (iii) competitive inhibition of the P-CheA·CheY interaction by unphosphorylated CheA. Our experimental measurements provided several kinetic parameters that can be related to the rate constants for the individual steps defined in eq 3. Measurements of $k_{observed}$ as a function of CheY concentration provided two kinetic parameters: (i) $k_{limiting}$, i.e., the limiting rate constant at saturating CheY concentration; (ii) K_m, i.e., the CheY concentration at which $k_{observed}$ was equal to half of $k_{limiting}$. Measurements of $k_{observed}$ as a function of the concentration of unphosphorylated CheA provided information (K_i) about the ability of unphosphorylated CheA to compete with P-CheA for the available CheY. Relating these to eq 3, $k_{limiting} = k_2$; $K_m = (k_{-1} + k_2)/k_1$; and $K_i = k_{-4}/k_4$ (i.e., the dissociation constant for the CheA·CheY complex). Li et al. (1995) measured a value of 6.7 μM for the K_d of the CheA:CheY-P complex, and this value would equal k_3/k_{-3} in eq 3. The reaction scheme presented in eq 3 will provide a framework for more detailed quantitative studies of the CheA−CheY phosphotransfer reaction and for investigations of the effects of various CheA and CheY mutations.

Kinetics of CheA−CheY Phosphotransfer: Significance in the Chemotaxis Signaling System. In vivo CheY concentrations have been estimated at ~8 μM (Kuo & Koshland, 1987), and our measurements indicated phosphotransfer proceeded with a $t_{1/2}$ of about 2 ms at this CheY concentration. The speed of this reaction reflects the relatively tight binding of CheY to P-CheA and the high rate constant for the subsequent chemical step that results in transfer of the phosphoryl group from His-48 of CheA to Asp-57 of CheY. Previous attempts to estimate the rate of phosphotransfer relied on steady-state measurements in which a coupled ATPase assay was used to monitor the flux of phosphate through the CheA−CheY reactions. However, computer simulations of this steady-state situation indicated that the assay is not particularly sensitive to the rate of CheA−CheY phosphotransfer when this reaction is considerably more rapid than CheA autophosphorylation and CheY autodephosphorylation. In addition, such ATP turnover assays may be complicated by the ability of unphosphorylated CheA to inhibit the CheA−CheY phosphotransfer reaction. Thus, the second-order rate constants reported for CheA−CheY phosphotransfer (12 μM^{-1} min^{-1}; Lukat et al., 1991) and for CheA−CheB phosphotransfer (25 μM^{-1} min^{-1}; Stewart, 1993) based on such steady-state measurements appear to grossly underestimate the actual rate constants that govern the phosphotransfer reactions. Furthermore, these values incorrectly imply that the kinetics of the phosphotransfer reactions can be described as simple second-order reactions.

It is informative to compare the rate of the CheA−CheY phosphotransfer reaction to the rates of the other reactions comprising the chemotaxis signal transduction pathway, although the kinetics of all these reactions have not been investigated in detail. We estimate[2] that CheA autophosphorylation could operate with a rate constant as high as 10−20 s^{-1}. With the rate constant governing the CheA−CheY phosphotransfer reaction expected to be at least 10 times faster than this, CheY-P would be generated at a rate limited by CheA's autophosphorylation rate. A similar conclusion was indicated by previous work (Borkovich et al., 1989; Ninfa et al., 1991). However, it is worth noting that only a fraction of the total CheA pool is expected to be in the 'receptor-coupled' state (Gegner et al., 1992; Borkovich & Simon, 1990); the rest of the CheA would presumably be free in the cytoplasm and would have such a low kinase activity that it would not contribute to the overall production of CheY-P; in fact, our results suggest that this uncoupled CheA would serve to inhibit the rate at which CheY can interact with receptor-coupled CheA. At sufficiently high levels of CheA, this inhibition can create situations in which CheY availability becomes a limiting factor in the ability of the system to generate CheY-P. More detailed and more informative modeling of the chemotaxis signal transduction system awaits the results of further detailed kinetic characterization of the phosphorylation and dephosphorylation reactions that operate in the chemotaxis signal transduction pathway.

Comparisons to Other Two-Component Phosphotransfer Systems. Only one other two-component system has been studied in detail at the kinetic level. Fisher et al. (1996) analyzed phosphotransfer from the kinase VanS to the response regulator proteins VanR and PhoB using rapid-reaction technology similar to that employed in our studies. The model we developed to describe the events involved in CheA−CheY phosphotransfer is similar in several respects

[2] In vitro results suggest that the CheA in an *E. coli* cell is found in two forms: receptor-coupled and uncoupled (Gegner et al., 1992). Only the coupled form (which would be expected to comprise ~50% of the total CheA) is expected to autophosphorylate sufficiently rapidly to contribute significantly to production of CheY-P. Borkovich et al. (1989) estimated that the rate of autophosphorylation of coupled CheA is ~300-fold faster than the rate of autophosphorylation of uncoupled CheA, while our own estimates suggest that this rate enhancement may be as high as ~800-fold. This latter value would indicate a rate constant of ~20 s^{-1} for autophosphorylation of receptor-coupled CheA.

to that described for the Van system: in both cases, there is kinetic evidence for formation of a complex involving the phospho-donor protein and the phospho-accepting protein prior to the chemical transfer of the phosphoryl group. The first-order rate constant for the chemical phosphotransfer step is considerably faster in the chemotaxis system ($k_2 \sim 650 \pm 200$ s^{-1}) than in the Van system ($k_2 \sim 1.6$ s^{-1}), perhaps reflecting the fact that the two systems have evolved to operate over very different time scales: the chemotaxis system must generate intracellular signals in less than 100 ms to appropriately modify the movements of a rapidly swimming cell, while the Van system serves to regulate gene expression over much more prolonged intervals. Our results indicated a relatively low K_m for the interaction of CheY with P-CheA (6.5 ± 2 μM), a situation that is also similar to that operating in the Van system ($K_m \sim 3$ μM). Another similarity between the Van and Che systems is the ability of the unphosphorylated form of the kinase to inhibit phosphotransfer by competing with the phosphorylated kinase for the available response regulator protein. Thus, the saturation kinetics and the inhibition of phosphotransfer by unphosphorylated kinase may be general characteristics of two-component signal transduction systems and should be taken into account in future attempts to model how such systems operate in vivo.

One aspect of the CheA−CheY interaction that appears to distinguish it from the VanR−VanS model is the reversibility of the phosphotransfer reaction. Lukat et al. (1990) previously suggested this reversibility for CheA and CheY, and our results have confirmed it. There is no evidence for reversibilty in the Van system (Fisher et al., 1996). Our results indicate that for the reversible reactions depicted in eq 3, the overall equilibrium constant (∼30−60) greatly favors phosphorylation of CheY in preference to CheA, but the reverse reaction can be detected under a variety of conditions. Indeed, our results demonstrate that the reverse reaction can take place on a fairly rapid time scale. It is not clear whether phosphotransfer from a response regulator to its cognate kinase is a common phenomenon for two-component systems, but it has also been observed in the OmpR/EnvZ system, where 'reverse phosphotransfer' may provide the mechanism by which the histidine protein kinase EnvZ also operates as a phosphatase that controls OmpR phosphorylation levels via dephosphorylation (Dutta & Inouye, 1996). This reversibility raises the possibility that systems or situations may exist in which phosphotransfer from the phosphoaspartate of a receiver module to the histidine of a transmitter module may play an important regulatory or signaling role. Indeed, several signal-transducing phospho-relay systems appear to make use of phosphotransfer from Asp to His (Posas et al., 1966; Tsuzuki et al., 1995; Uhl & Miller, 1996).

Two-component signal transduction pathways are ubiquitous, playing key roles in prokaryotes, eukaryotes, and archaeons (Alex & Simon, 1994; Parkinsin & Kofoid, 1992; Rudolph et al., 1995). The components of such pathways, in particular the proteins comprising the bacterial chemotaxis signal transduction pathway, have been studied using a variety of different biochemical approaches. However, at present little information is available about the kinetics of the interaction of the proteins involved in the phosphotransfer reaction and the kinetics of the phosphotransfer event itself. Therefore, our results not only serve to define the kinetics of the interaction between P-CheA and CheY in the bacterial chemotaxis system, but may also provide information useful for constructing a general working model of kinase−response regulator interactions in two-component systems.

ACKNOWLEDGMENT

I thank K. Clark and the reviewers for helpful comments on the manuscript, J. S. Parkinson for providing strains and plasmids, and R. VanBruggen for cheerful technical assistance in protein purifications and SDS−PAGE analysis of large numbers of quench-flow samples. A. Evagelidis and C.-X. Huang assisted in determining the quenching conditions used in this work and in determining the appropriate time scales for observation.

REFERENCES

Alex, L., & Simon, M. I. (1994) *Trends Genet. 10*, 133−138.
Berg, H. C., & Brown, D. A. (1972) *Nature 239*, 500−504.
Berg, H. C., & Tedesco, P. M. (1975) *Proc. Natl. Acad. Sci. U.S.A. 72*, 3235−3239.
Bevington, P. R. (1969) in *Data Reduction and Error Analysis for the Physical Sciences*, McGraw-Hill, New York.
Block, S. M., Segall, J. E., & Berg, H. C. (1982) *Cell 31*, 215−226.
Boerner, R. J., Kassel, D. B., Edison, A. M., & Knight, W. B. (1995) *Biochemistry 34*, 14852−14860.
Borkovich, K. A., & Simon, M. I. (1990) *Cell 63*, 1339−1348.
Borkovich, K. A., Kaplan, N., Hess, J. F., & Simon, M. I. (1989) *Proc. Natl. Acad. Sci. U.S.A. 86*, 1208−1212.
Borkovich, K. A., Alex, L. A., & Simon, M. I. (1992) *Proc. Natl. Acad. Sci. U.S.A. 89*, 6756−6760.
Bourret, R. B., Hess, J. F., & Simon, M. I. (1990) *Proc. Natl. Acad. Sci. U.S.A. 87*, 41−45.
Bourret, R. B., Borkovich, K. A., & Simon, M. I. (1991) *Annu. Rev. Biochem. 60*, 401−441.
Bourret, R. B., Drake, S. K., Chervitz, S. A., Simon, M. I., & Falke, J. J. (1993) *J. Biol. Chem. 268*, 13089−13096.
Bray, D., & Bourret, R. B. (1995) *Mol. Biol. Cell 6*, 1367−1380.
Bray, D., Bourret, R. B., & Simon, M. I. (1993) *Mol. Biol. Cell 4*, 469−482.
Drake, S. K., Bourret, R. B., Luck, L. A., Simon, M. I., & Falke, J. J. (1993) *J. Biol. Chem. 268*, 13081−13088.
Dutta, R., & Inouye, M. (1996) *J. Biol. Chem. 271*, 1424−1429.
Evagelidis, A. (1995) M.S. thesis, McGill University.
Fisher, S. L., Kim, S.-K., Wanner, B. L., & Walsh, C. T. (1996) *Biochemistry 35*, 4732−4740.
Fukami, Y., & Lipmann, F. (1983) *Proc. Natl. Acad. Sci. U.S.A. 80*, 1872−1876.
Gegner, J. A., Graham, D. R., Roth, A. F., & Dahlquist, F. W. (1992) *Cell 18*, 975−982.
Gill, S. C., & von Hippel, P. H. (1989) *Anal. Biochem. 182*, 319−326.
Gutfreund, H. (1969) *Methods Enzymol. 16*, 229−249.
Hauri, D. C., & Ross, J. (1995) *Biophys. J. 68*, 708−722.
Hess, J. F., Oosawa, K., Matsumura, P., & Simon, M. I. (1987) *Proc. Natl. Acad. Sci. U.S.A. 84*, 7609−7613.
Hess, J. F., Bourret, R. B., Oosawa, K., Matsumura, P., & Simon, M. I. (1988a) *Cold Spring Harbor Symp. Quant. Biol. 53*, 41−48.
Hess, J. F., Bourret, R. B., & Simon, M. I. (1988b) *Nature 336*, 139−143.
Hess, J. F., Oosawa, K., Kaplan, N., & Simon, M. I. (1988c) *Cell 53*, 79−87.
Huang, C.-X., & Stewart, R. C. (1993) *Biochim. Biophys. Acta 1202*, 297−304.
Hubler, L., Gill, G. N., & Bertics, P. J. (1989) *J. Biol. Chem. 264*, 1558−1564.
Khan, S., Castellano, F., Spudich, J. L., McCray, J. A., Goody, R. S., Reid, G. P., & Trentham, D. R. (1993) *Biophys. J. 65*, 2368−2382.
Kole, H. K., Abdel-Ghany, M., & Racker, E. (1988) *Proc. Natl. Acad. Sci. U.S.A. 85*, 5849−5853.

Kuo, S. C., & Koshland, D. E., Jr. (1987) *J. Bacteriol. 169*, 1307−1314.
Kwiatkowski, A. P., Huang, C. Y., & King, M. M. (1990) *Biochemistry 29*, 153−159.
Li, J., Swanson, R. V., Simon, M. I., & Weis, R. M. (1995) *Biochemistry 34*, 14626−14636.
Lowry, D. F., Roth, A. F., Rupert, P. B., Dahlquist, F. W., Moy, F. J., Domaille, P. J., & Matsumura, P. (1994) *J. Biol. Chem. 269*, 26358−26362.
Lukat, G. S., Stock, A. M., & Stock, J. B. (1990) *Biochemistry 29*, 5436−5442.
Lukat, G. S., Lee, B. H., Mottonen, J. M., Stock, A. M., & Stock, J. B. (1991) *J. Biol. Chem. 266*, 8348−8354.
Lukat, G. S., McCleary, W. R., Stock, A. M., & Stock, J. B. (1992) *Proc. Natl. Acad. Sci. U.S.A. 89*, 718−722.
McCleary, W. R., & Stock, J. B. (1994) *J. Biol. Chem. 269*, 31567−31572.
McEnvoy, M. M., Zhou, H., Roth, A. F., Lowry, D. F., Morrison, T. B., Kay, L. E., & Dahlquist, F. W. (1995) *Biochemistry 34*, 13871−13880.
Morrison, T. B., & Parkinson, J. S. (1994a) *BioTechniques 17*, 922−926.
Morrison, T. B., & Parkinson, J. S. (1994b) *Proc. Natl. Acad. Sci. U.S.A. 91*, 5485−5489.
Ninfa, E. G., Stock, A., Mowbray, S., & Stock, J. (1991) *J. Biol. Chem. 266*, 9764−9770.
Parkinson, J. S., & Kofoid, E. C. (1992) *Annu. Rev. Genet. 26*, 71−112.
Pickard, C., & Jencks, W. P. (1984) *J. Biol. Chem. 259*, 1629−1643.
Rudolph, J., Tolliday, N., Schmitt, C., Schuster, S. C., & Oesterhelt, D. (1995) *EMBO J. 14*, 4249−4257.
Sanders, D. A., Gillece-Castro, B. L., Stock, A. M., Burlingame, A. L., & Koshland, D. E., Jr. (1989) *J. Biol. Chem. 264*, 21770−21778.
Segall, J. E., Manson, M. D., & Berg, H. C. (1982) *Nature 296*, 855−857.
Shizuta, Y., Beaveo, J. A., Bechtel, P. J., Hofmann, F., & Krebs, E. G. (1975) *J. Biol. Chem. 250*, 6891−6896.
Shukla, D., & Matsumura, P. (1995) *J. Biol. Chem. 270*, 24414−24419.
Stewart, R. C. (1993) *J. Biol. Chem. 268*, 1921−1930.
Stock, A. M., Wylie, D. C., Mottonen, J. M., Lupas, A. M., Ninfa, E. G., Ninfa, A. J., Schutt, C. E., & Stock, J. B. (1988) *Cold Spring Harbor Symp. Quant. Biol. 53*, 49−57.
Stock, J., & Surette, M. G. (1996) In *Escherichia coli and Salmonella. Cellular and Molecular Biology* (Neidhardt, F. C., Ed.) pp 1103−1129, ASM Press, Washington, D.C.
Strickland, S., Palmer, G., & Massey, V. (1975) *J. Biol. Chem. 250*, 4048−4052.
Studier, F. W., et al. (1990) *Methods Enzymol. 185*, 60−89.
Surette, M. G., Levit, M., Liu, Y., Lukat, G., Ninfa, E. G., Ninfa, A., & Stock, J. B. (1996) *J. Biol. Chem. 271*, 939−945.
Swanson, R. V., Bourret, R. B., & Simon, M. I. (1993a) *Mol. Microbiol. 8*, 435−441.
Swanson, R. V., Schuster, S. C., & Simon, M. I. (1993b) *Biochemistry 32*, 7623−7629.
Tawa, P., & Stewart, R. C. (1994) *Biochemistry 33*, 7917−7924.
Tsuzuki, M., Ishige, K., & Mizuno, T. (1995) *Mol. Microbiol. 18*, 953−962.
Uhl, M. A., & Miller, J. F. (1996) *EMBO J. 15*, 1028−1036.
Welch, M., Oosawa, K., Aizawa, S.-I., & Eisenbach, M. (1994) *Biochemistry 33*, 10470−10476.
Wolfe, A. J., & Stewart, R. C. (1993) *Proc. Natl. Acad. Sci. U.S.A. 90*, 1518−1522.
Wylie, D., Stock, A., Wong, C.-Y., & Stock, J. (1988) *Biochem. Biophys. Res. Commun. 151*, 891−896.

BI962261K